Capacity Analysis of RIS-based Communications Under Transceiver Impairments

Waqas Khalid
Institute of Industrial Technology
Korea University
Sejong 30019, South Korea
waqas283@korea.ac.kr

Heejung Yu
Department of Electronics and Information Engineering
Korea University
Sejong 30019, South Korea
heejungyu@korea.ac.kr

***Abstract*—In this paper, we consider a reconfigurable intelligent surface (RIS)-aided wireless communication without a direct link. The large-scale path loss model, and residual hardware impairment (RHI), taking into account the physical characteristics of RIS, and practical nature of transceiver equipment, respectively, are considered. By employing the Rayleigh distribution for small-scale fading and the central limit theorem (CLT) approximation for number of reflecting surfaces, we derive the distribution of SNR, and consequently, the tractable expression of ergodic achievable rate for the analysis. We analyze the factors, including effective incident angle and size of RIS, and number of reflecting surfaces, and RHI Level, that influence the ergodic achievable rate, by simulation results.**

***Index Terms*—reconfigurable intelligent surface, hardware impairments, ergodic achievable rate**

I. Introduction

Reconfigurable intelligent surface (RIS) is a new technology to enable energy-, spectrum-, and cost-efficient wireless communications [1]. In this paper, we consider an RIS-assisted downlink wireless system. In particular, we include the realistic path loss model for RIS-assisted wireless system employing the physical characteristics of RIS, e.g., its effective angle of incident and size, in contrast to expressing only the function of link distance for large-scale fading. Furthermore, the assumption of ideal hardware components is also not realistic in practical communication systems. The transceivers in practice suffer from various hardware impairments, such as phase noise, and in-phase/quadrature-phase imbalance, which cannot be completely removed [2]. Therefore, we consider the residual hardware impairments (RHI) characteristics. We aim to quantify the ergodic achievable rate (ER) performance of the proposed analysis. We derive the distribution of signal-to-noise-plus-interference ratio (SNIR) and closed-form expression of ER. Finally, the numerical results are presented to validate the analytical expressions and also to show useful insights on the impact of different parameters.

This work was supported in part by the National Research Foundation of Korea (NRF) grant funded by the Korean government (MSIT; 2019R1A2C1083988), and in part by the MSIT, Korea under the Information Technology Research Center (ITRC) support program (IITP-2021-2016-0-00313) supervised by the Institute for Information and communications Technology Promotion (IITP).

II. System Model

We consider an RIS-aided wireless system including a base-station (S), and a user (U). The direct link between S and U does not exist due to obstruction. The RIS with T number of passive reflecting elements aims to constructively add-up signals at U. The more suitable large-scale path loss model for RIS can be considered as $P_L = \frac{G_T}{16\pi^2}\left(\frac{xy}{d_s d_u}\right)^2 cos^2\left(\theta_t\right)$, where G_T represents the effective gain of the antennas, θ_t represents the effective incident angle; the angle between the incident and normal directions when RIS plane is vertically straight. d_s, and d_u are the distances between S and t element, and t element and U, respectively, $x \times y$ is the size and $xycos\left(\theta_t\right)$ is the effective area for the beam on RIS. We consider the far-field transmission for S and U. For small-scale fading, the channels between S and t element, and t element and U, are represented as $h_t = \alpha_t e^{j\theta_t}$, and $g_t = \beta_t e^{j\epsilon_t}$, respectively, where h_t, and g_t are the amplitudes following the Rayleigh distribution, and $|h_t|^2$, and $|g_t|^2$ are the channel gains following the exponential distribution with with scale parameter equal to 1 [3], [4].

The received signal at U is,

$$Y = \sqrt{P_L}\sum_{t=1}^{T} h_t \Theta_t g_t \left(\sqrt{P_T}X + \nu_T\right) + n_D \tag{1}$$

where P_T is the transmit power at S, X is the unit signal, and $n_D \dot{\sim} \mathcal{CN}\left(0, \sigma^2\right)$ is AWGN [5]. $\Theta_t = \psi_t e^{j\phi_t}$, $\phi_t \in [-\pi, \pi)$, and $\psi_t = [0, 1]$ are the induced reflection coefficient, phase shift, and amplitude for the t element of RIS. The aggregate RSI noise, $\nu_T \dot{\sim} \mathcal{CN}\left(0, \sigma_T^2 P_T\right)$, is sum of the effective distortion noises ν_S and $\frac{\nu_U}{\Omega}$. In details, $\Omega = |\sum_{t=1}^{T} h_t \Theta_t g_t|^2$ is the effective instantaneous channel gain, $\nu_S \dot{\sim} \mathcal{CN}\left(0, \sigma_S^2 P_T\right)$, and $\nu_U \dot{\sim} \mathcal{CN}\left(0, \sigma_U^2 P_T \Omega\right)$ are the RHI noises at S and U, respectively. $\sigma_T = \sqrt{\sigma_S^2 + \sigma_U^2}$ represents the aggregate level of RHI.

Using $\rho_T = \frac{P_T}{\sigma^2}$, the SINR at U is,

$$\gamma = \frac{P_L |\sum_{t=1}^{T} \alpha_t \beta_t e^{(\theta_t + \epsilon_t + \phi_t)} \psi_t|^2 \rho_T}{P_L \sum_{t=1}^{T} \alpha_t \beta_t e^{(\theta_t + \epsilon_t + \phi_t)} \psi_t|^2 \rho_T \sigma_T^2 + 1} \tag{2}$$

We consider that the channel state information (CSI) is known at RIS, and the optimal setting, i.e., $\phi_t = \theta_t + \epsilon_t$, and

$\psi_t = 1$, is possible. Therefore, the SNR at U can be rewritten as $\gamma = \frac{\Omega^2 \gamma_a}{\Omega^2 \gamma_b + 1}$, where $\Omega = \sum_{t=1}^{T} \alpha_t \beta_t$, $\gamma_a = P_L \rho_T$, and $\gamma_b = P_L \rho_T \sigma_T^2$.

III. Ergodic Rate Analysis

We present the statistical characterization of Ω. α_t, and β_t follow the Rayleigh distribution. According to the central limit theorem (CLT), $\Omega = \sum_{t=1}^{T} \alpha_t \beta_t$ can be approximated with a Gaussian distributed $\mathcal{RV}$ for a sufficiently large T. The mean value $\mathbb{E}\{\Omega\}$ and variance $\mathbb{V}\{\Omega\}$ can be expressed as $T\frac{\pi}{4}$ and $T\left(\frac{16-\pi^2}{16}\right)$, respectively. Now, we find the exact first and second moments of Ω^2. The first moment $\mathbb{E}\{\Omega^2\}$ of Ω^2 can be written as,

$$\begin{aligned} \mathbb{E}\{\Omega^2\} &= \mathbb{V}\{\Omega\} + (\mathbb{E}\{\Omega\})^2 \\ &= T\left(\frac{16-\pi^2}{16}\right) + \left(T\frac{\pi}{4}\right)^2 \end{aligned} \quad (3)$$

The second moment $\mathbb{E}\{\Omega^4\}$ of Ω^2 can be determined as,

$$\begin{aligned} \mathbb{E}\{\Omega^4\} &= (\mathbb{E}\{\Omega\})^4 + 6\,(\mathbb{E}\{\Omega\})^2\,\mathbb{V}\{\Omega\} + 3\,(\mathbb{V}\{\Omega\})^2 \\ &= \left(T\frac{\pi}{4}\right)^4 + 6\left(T\frac{\pi}{4}\right)^2 T\left(\frac{16-\pi^2}{16}\right) \\ &+ 3\left(\frac{T\left(16-\pi^2\right)}{16}\right)^2 \end{aligned} \quad (4)$$

We get $\Omega \dot{\sim} \Gamma\left(k_\Omega, \theta_\Omega\right)$ using moment-matching technique, where the shape and scale parameters are respectively obtained as $k_\Omega = \frac{\mathbb{E}\{\Omega\}^2}{\mathbb{V}\{\Omega\}}$, and $\theta_\Omega = \frac{\mathbb{V}\{\Omega\}}{\mathbb{E}\{\Omega\}}$. The ergodic rate is determined as $ER = \mathbb{E}\left\{\log_2\left(1+\frac{\Omega\gamma_a}{\Omega\gamma_b+1}\right)\right\}$, which is solved using the approximation $\mathbb{E}\left\{\log_2\left(1+\frac{q_1}{q_2+1}\right)\right\} \approx \frac{1}{\ln 2}\ln\left(1+\frac{\mathbb{E}\{q_1\}}{\mathbb{E}\{q_2\}+1}\right)$ [6].

The ergodic rate can be rewritten as,

$$ER \approx \frac{1}{\ln 2}\ln\left(1+\frac{\mathbb{E}\left\{\Omega\gamma_a\right\}}{\mathbb{E}\left\{\Omega\gamma_b\right\}+1}\right), \quad (5)$$

where $\mathbb{E}\left\{\Omega\gamma_a\right\} = \gamma_a k_\Omega \theta_\Omega$, and $\mathbb{E}\left\{\Omega\gamma_b\right\} = \gamma_b k_\Omega \theta_\Omega$.

IV. Numerical Results

The provided numerical results confirm the theoretical analysis. The parameters are set as; transmit SNR ρ_T = [0dB, 20dB], RHI level $\sigma_T = [0, 0.3]$, number of reflecting elements $T = [20, 80]$, length of reflecting element l_r = [$\frac{\lambda}{6}$, λ], where xy = Tl_r^2, and effective incident angle of RIS θ_t = [$\frac{\pi}{6}$, $\frac{3\pi}{4}$].

Fig. 2(a) plots ER performance versus ρ_T, for different θ_t, and l_r. The ER performance improves with ρ_T. Further, increase in θ_t degrades the ER performance as $\cos\left(\theta_t\right)$ corresponds to the effective impinging area for the incident wave on RIS. The results also show that ER increases with l_r, as the total area of RIS become larger with l_r when T is fixed. Fig. 2(b) plots ER performance versus ρ_T, for different T, and σ_T. First, the results confirm that T has a positive impact on the ER performance as larger passive beamforming gain can be achieved. The results also show that ER decreases, i.e., the reliability degrades, with the increase in ζ_T. The reason is that RHI level has a negative impact on the ER performance. For the comparison, the ideal case of RHI, i.e., ζ_T = 0, is shown. The results demonstrate that the impact of ζ_T is more severe for the higher SNR.

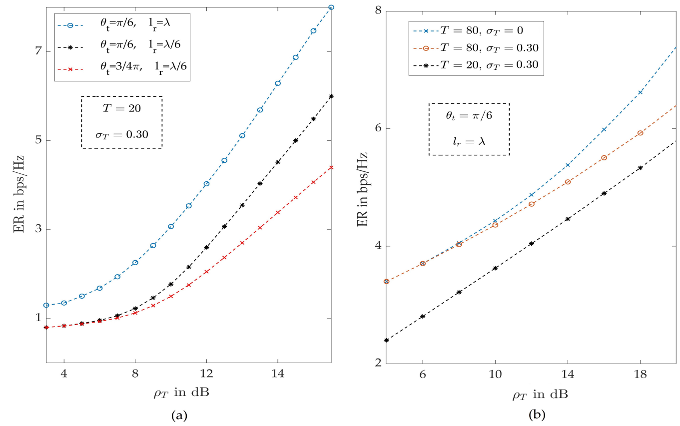

Fig. 1. a) ER performance versus ρ_T for different θ_t, and l_r b) ER performance versus ρ_T for different T, and σ_T.

V. Conclusion

In the paper, we investigate the reconfigurable intelligent surface (RIS) technology to enhance the reliability performance of the RIS-aided wireless system, and derive the closed-form analytical expression for the ergodic achievable rate. To design the practical setup, we consider the non-ideal hardware impairments, and realistic large-scale path loss model employing the physical characteristics of RIS. The results illustrate the correctness of the analytical analysis. The performance of ergodic achievable rate was examined for different variables, including size and angle incident for RIS, RHI level, and number of reflecting elements.

References

[1] A. A. Boulogeorgos, A. Alexiou, "Performance analysis of reconfigurable intelligent surface-assisted wireless systems and comparison with relaying," *IEEE Access*, vol. 8, pp. 94463–94483, May 2020.

[2] Li et al., "Joint effects of residual hardware impairments and channel estimation errors on SWIPT assisted cooperative NOMA networks," *IEEE Access*, vol. 7, pp. 135499–135513, Sept. 2019.

[3] W. Khalid, H. Yu, S. Noh, "Residual energy analysis in cognitive radios with energy harvesting UAV under reliability and secrecy constraints," *Sensors*, vol. 20, no. 10, pp. 2998–3016, May 2020.

[4] W. Khalid, H. Yu, "Spatial–temporal sensing and utilization in full duplex spectrum-heterogeneous cognitive radio networks for the internet of things," *Sensors*, vol. 19, no. 6, pp. 1441–1458, May 2020.

[5] W. Khalid, H. Yu, "Security improvement With QoS provisioning using service priority and power allocation for NOMA-IoT networks," *IEEE Access*, vol. 9, pp. 9937–9948, Jan. 2021.

[6] H. Y, I. G. Lee, "Physical layer security based on NOMA and AJ for MISOSE channels with an untrusted relay," *Future Generation Computer Systems*, vol. 102, pp. 611–618, Jan. 2020.